

Direct Signaling from Astrocytes to Neurons in Cultures of Mammalian Brain Cells

Maiken Nedergaard

Although astrocytes have been considered to be supportive, rather than transmissive, in the adult nervous system, recent studies have challenged this assumption by demonstrating that astrocytes possess functional neurotransmitter receptors. Astrocytes are now shown to directly modulate the free cytosolic calcium, and hence transmission characteristics, of neighboring neurons. When a focal electric field potential was applied to single astrocytes in mixed cultures of rat forebrain astrocytes and neurons, a prompt elevation of calcium occurred in the target cell. This in turn triggered a wave of calcium increase, which propagated from astrocyte to astrocyte. Neurons resting on these astrocytes responded with large increases in their concentration of cytosolic calcium. The gap junction blocker octanol attenuated the neuronal response, which suggests that the astrocytic-neuronal signaling is mediated through intercellular connections rather than synaptically. This neuronal response to local astrocytic stimulation may mediate local intercellular communication within the brain.

The central nervous system is composed of an intimately associated network of neurons and astrocytes (1). Despite the central importance of an interaction between these two cell types, only recently have studies suggested that astrocytic functions might not be limited to the structural and trophic support of neurons. Astrocytes display rapid electrical responses to neuronal activity, and intense neuronal activity can trigger slowly propagating astrocytic Ca^{2+} waves (2). Similarly, Schwann cells at the neuromuscular junction and glial cells along the optical nerve show increased concentrations of cytosolic calcium ($[Ca^{2+}]_i$) in response to neuronal activity (3). In addition, cultured astrocytes show both oscillatory Ca^{2+}_i responses and propagating Ca^{2+} waves in response to glutamate application as well as mechanical stimulation (4). However, astrocytes have not previously been shown to influence neuronal activity.

To investigate communication between cocultured neurons and astrocytes, I stimulated single astrocytes and examined Ca^{2+}_i responses in the surrounding cells using the fluorescent calcium indicator fluo-3 (5). A focally applied electric field evoked a marked increase in $[Ca^{2+}]_i$, which was initially restricted to the target astrocyte (6). In confluent cultures, this was followed by an increase in $[Ca^{2+}]_i$ in neighboring astrocytes, and a wave of astrocytic increase in $[Ca^{2+}]_i$ then evolved that often spread beyond the field of view (velocity = $20 \pm 8 \mu\text{m/s}$). Similar Ca^{2+} waves could also be elicited by either mechanical or laser stimulation of single astrocytes (6). The Ca^{2+} waves evoked by these distinct stimulation paradigms did not differ from one another

or from the propagating Ca^{2+} waves described previously after glutamate exposure (4).

Neurons lying on a contiguous monolayer of astrocytes, through which the Ca^{2+} wave propagated, increased their $[Ca^{2+}]_i$ (Table 1). Neuronal $[Ca^{2+}]_i$ increased only in neurons that were in physical contact with astrocytes participating in the Ca^{2+} wave. Indeed, it was sufficient for induction of a neuronal $[Ca^{2+}]_i$ response that only a neurite was in contact with the wave: cell body contact per se was not necessary (Fig. 1). In contrast, neurons plated directly on the fibronectin substrate layer or on astrocytes not participating in the wave did not react to field potentials (Fig. 1). The mean time to reaction was approximately 12.4 ± 7.8 s (mean \pm SD; range, 3 to 36 s; $n = 120$) after termination of the electric stimulation. Reaction time was dependent on the distance to the stimulation site [corre-

lation coefficient (r) = 0.65, $P < 0.0001$]. Upon contact with the wave, neuronal $[Ca^{2+}]_i$ increased rapidly: within 2.40 ± 1.25 s (range, 0 to 7 s), a maximal elevation of $369 \pm 274\%$ (range, 42 to 1185%) above the base line was detected, which normalized within 5 to 10 min. Most neurons in physical contact with the propagating astrocytic Ca^{2+} waves responded (120 out of 131 neurons examined in 10 experiments). Repeated stimulation of the same target astrocyte typically evoked identical patterns and magnitude of increases in $[Ca^{2+}]_i$ in astrocytes as well as in neurons. The maximal radius over which the astrocytic Ca^{2+} wave spread, and the velocity with which it migrated, were not affected by the coculturing of neurons (Table 1).

Neurons were tentatively identified during the experiments as cells with round, phase-bright and nongranulated cell bodies, with relatively unbranched processes. Retrospectively, we verified neuronal identity by immunostaining for microtubule-associated protein 2 (MAP-2) (7). Astrocytes were similarly identified by staining for glial fibrillary acidic protein (GFAP) (7).

To test whether the Ca^{2+} wave was transmitted by extracellular release and diffusion of an astrocyte-derived substance, I evoked intercellular Ca^{2+} signaling during rapidly flowing solution changes. Superfusion with a linear velocity vector opposite to and 20 times faster than the Ca^{2+} wave did not affect signaling, either between astrocytes or between astrocytes and neurons (8). Although these observations do not exclude the possibility that signaling is mediated by intercellular diffusion of a humoral agent, the constancy of both the direction and velocity of wave propagation over a range of perfusion rates suggests otherwise.

To examine whether the Ca^{2+} signaling

Table 1. Effects of pharmacological inhibition. Shown is the mean \pm SD; four to ten experiments per treatment condition were performed. N.A., not applicable.

Treatment	Radius (μm)	Velocity ($\mu\text{m/s}$)	Neurons activated (%)	$\Delta F/F$ (%)	Total neurons
<i>Glial cultures</i>					
Untreated	250 ± 50	20 ± 8	N.A.	N.A.	N.A.
<i>Mixed cultures</i>					
Untreated	257 ± 66	19 ± 9	92	369 ± 274	131
TTX	252 ± 89	26 ± 16	88	363 ± 229	51
AP-5	272 ± 148	31 ± 15	95	512 ± 225	97
MK-801	221 ± 54	20 ± 17	89	435 ± 417	54
NBQX	270 ± 85	24 ± 14	88	360 ± 216	58
Kynurenic acid + TTX	285 ± 54	27 ± 13	86	397 ± 285	72
	264 ± 55	24 ± 12	85	478 ± 315	75
Nifedipine	298 ± 57	18 ± 8	92	384 ± 244	63
Calcium-free + TTX	294 ± 113	22 ± 15	93	360 ± 239	67
	251 ± 67	21 ± 11	89	331 ± 161	57
Octanol	10 ± 5	N.A.	0	N.A.	60
Halothane	15 ± 6	N.A.	0	N.A.	70

Aitken Neurosurgery Laboratory, Division of Neurosurgery, Department of Surgery, Cornell University Medical College, 1300 York Avenue, New York, NY 10021, USA.

occurred through a synaptical mechanism, I applied 1 μM tetrodotoxin (TTX), the Na^+ channel blocker (9). Tetrodotoxin had no effect on the amplitude of $[\text{Ca}^{2+}]_i$ increase or on the velocity or distance of spread in either neurons or astrocytes (Table 1). I also tested astrocyte-to-neuron signaling in the presence of a variety of selective glutamate receptor antagonists, which included 2-amino-5-phosphonopentanoic acid (AP-5) (1 mM), 2,3-dihydroxy-6-nitro-7-sulfamoylbenzo(f)-quinoxaline (NBQX) (50 μM), and MK-801 (10 μM), none of which had any measurable effect on the wave (Table 1). In addition,

signaling from astrocytes to neurons remained unaffected by the unselective glutamate receptor antagonist kynurenic acid: When the astrocytic Ca^{2+} wave was evoked by the electric field potential, it propagated from astrocytes to astrocytes with a velocity of $27 \pm 13 \mu\text{m/s}$ in the presence of 2 mM kynurenic acid (eight experiments) and activated 62 of 72 neurons. This is of particular note because kynurenic acid has been reported to block all astrocytic responses to neuronal stimulation (3), and the same concentration of kynurenic acid completely blocked neuronal responses to application of 100 μM glutamate (22 neurons in

three experiments). Kynurenic acid and TTX together also failed to inhibit astrocytic signaling to neurons (Fig. 2 and Table 1). The I-type Ca^{2+} channel blocker nifedipine influenced neither the vectorial progression of the Ca^{2+} wave nor its extent of neuronal activation (Table 1). Similarly, I confirmed earlier observations that depletion of extracellular Ca^{2+} did not affect the astrocytic Ca^{2+} wave (4). Accordingly, the astrocytic signaling to neurons also was not diminished by removal of extracellular Ca^{2+} (Table 1). Taken together, these results suggest that the elevations in $[\text{Ca}^{2+}]_i$ in both astrocytes and neu-

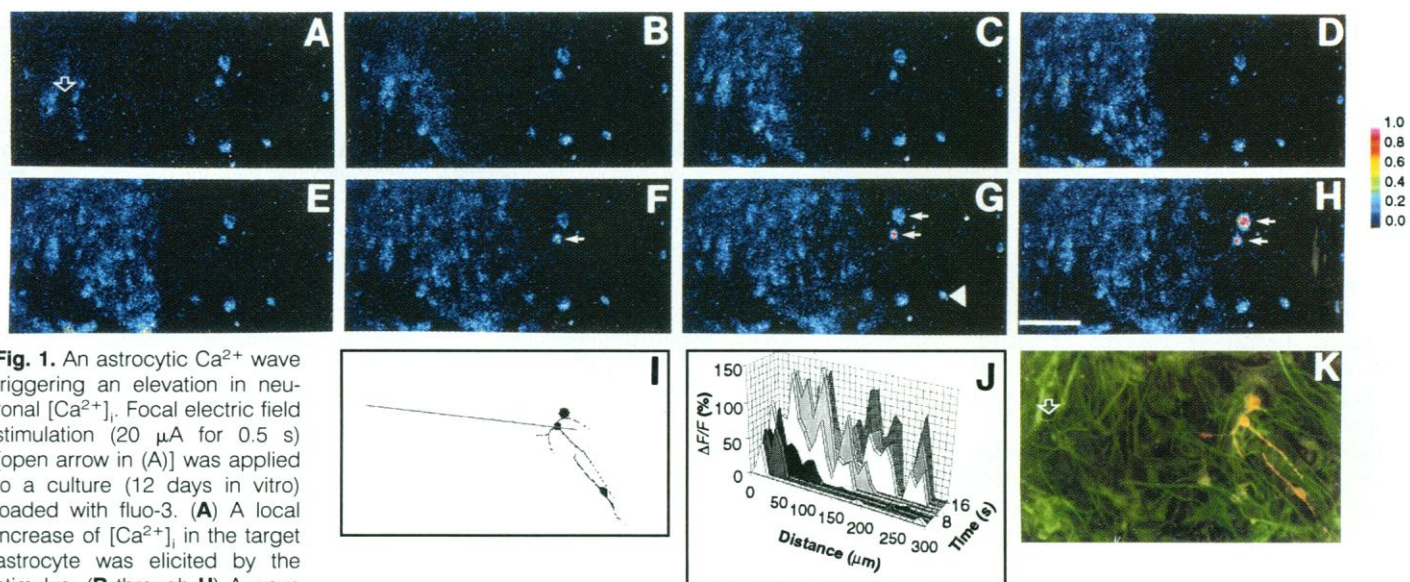
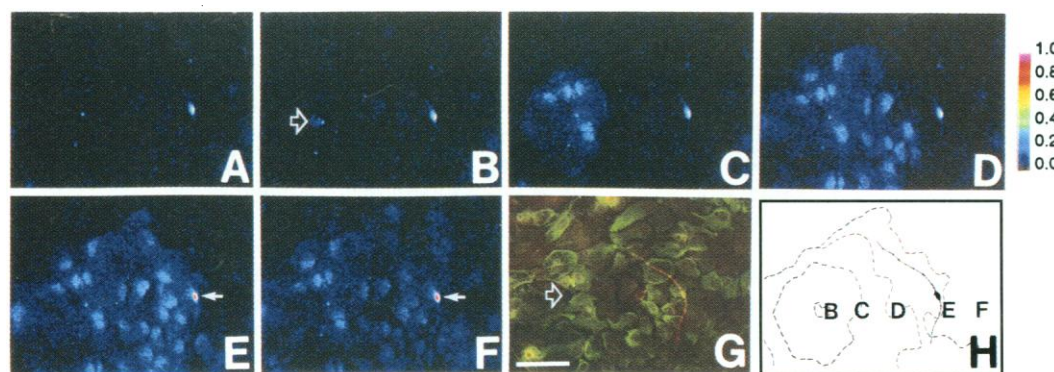


Fig. 1. An astrocytic Ca^{2+} wave triggering an elevation in neuronal $[\text{Ca}^{2+}]_i$. Focal electric field stimulation (20 μA for 0.5 s) [open arrow in (A)] was applied to a culture (12 days in vitro) loaded with fluo-3. (A) A local increase of $[\text{Ca}^{2+}]_i$ in the target astrocyte was elicited by the stimulus. (B through H) A wave of increase in $[\text{Ca}^{2+}]_i$ propagated to include the surrounding astrocytes and neurons. Small arrows (F through H) identify neurons with elevated $[\text{Ca}^{2+}]_i$. The concentration of Ca^{2+} remained at resting values in the neuron in (G) (arrowhead), which was not in direct physical contact with the Ca^{2+} wave. Images were captured at 2-s intervals, beginning 2 s after electric field stimulation. (I) A schematic diagram of the three MAP-2-positive neurons in the field. Relative changes in emission ($\Delta F/F$) were measured along the line indicated. (J) Traces showing the fluorescence shifts ($\Delta F/F$) along the line

indicated in (I) as a function of time. (K) Immunodetection of the neuronal-glia antigens, MAP-2 and GFAP, respectively, within this field. GFAP-positive astrocytes (fluorescein tagged secondary) form a confluent layer. The three MAP-2-positive neurons (Texas red tagged secondary) are lying on this astrocytic substrate layer. Only the top two neurons were in contact with subjacent astrocytes participating in the Ca^{2+} wave. The scale indicates the relative emission intensity of the Ca^{2+} indicator fluo-3. Scale bar, 100 μm .

Fig. 2. Waves of astrocytic Ca^{2+} in elevated concentrations propagate and trigger elevations in neuronal $[\text{Ca}^{2+}]_i$, despite the presence of 1 μM TTX and 2 mM kynurenic acid. (A) An 18-day in vitro culture loaded with fluo-3. (B through F) Electric field stimulation (open arrow) (15 μA for 0.5 s) triggers a local elevation of astrocytic $[\text{Ca}^{2+}]_i$. The images shown were captured 1, 4, 7, 10, and 26 s, respectively, after electrical field stimulation (small arrow identifies the neuron as $[\text{Ca}^{2+}]_i$ rises). Elevations in neuronal $[\text{Ca}^{2+}]_i$ were first noted when the neuron was approached by the astrocytic Ca^{2+} wave. Thus, TTX and kynurenic acid did not block intercellular signaling, either between astrocytes or from astrocytes to neurons. (G) Detection of MAP-2 and GFAP immunoreactivity in the same field. (H)



Line drawing illustrating propagation of the astrocytic Ca^{2+} wave, from (B) through (F). The MAP-2-positive neuron in the field is outlined. The scale indicates the relative emission intensity of the Ca^{2+} indicator fluo-3. Scale bar, 100 μm .

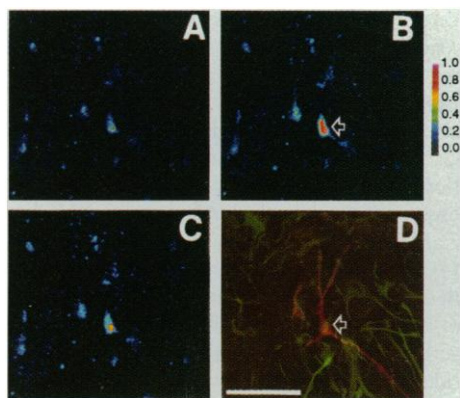


Fig. 3. Signaling between astrocytes and neurons is unidirectional. **(A)** Resting fluo-3 signal of a culture 10 days in vitro. **(B)** Direct stimulation of a neuron ($4 \mu\text{A}$ for 0.5 s) (open arrow) evoked a large increase in neuronal $[\text{Ca}^{2+}]_i$ (2 s), but an astrocytic Ca^{2+} wave was not evoked (2 min). **(C)** Detection of MAP-2 and GFAP immunoreactivity in the same field as in **(A)** through **(C)**. The scale indicates the relative emission intensity of the Ca^{2+} indicator fluo-3. Scale bar, $100 \mu\text{m}$.

rons derived from the release of intracellular stores of Ca^{2+} (4). Also, because the presence of extracellular Ca^{2+} is essential for the release of neurotransmitters (10), wave propagation is further unlikely to be dependent on synaptic transmission.

I also tested whether Ca^{2+} signaling can occur in the opposite direction, from neuron to astrocyte. Single neurons resting on continuous layers of astrocytes were stimulated directly by an electric field potential. A maximal increase of $347 \pm 252\%$ ($n = 17$) (range, 97 to 1106%) of neuronal $[\text{Ca}^{2+}]_i$ was not sufficient to trigger astrocytic Ca^{2+} waves (Fig. 3). Thus, these observations indicate that signaling between astrocytes and neurons is unidirectional. In accordance with prior reports (4), gap junctions were required for interastrocytic Ca^{2+} signaling: Each of the gap junction blockers halothane and octanol blocked the astrocytic Ca^{2+} wave. In addition, signaling from astrocytes to neurons was inhibited: when exposed to octanol, stimulated astrocytes in direct physical contact with neurons failed to evoke an increase in neuronal $[\text{Ca}^{2+}]_i$ ($n = 9$) (Fig. 4 and Table 1). The neuronal $[\text{Ca}^{2+}]_i$ response to glutamate exposure was not reduced in the presence of equal concentrations of halothane or octanol (11).

I further tested whether cultured neurons possess functional gap junctions by evaluating the recovery of intracellular fluorescence after photobleaching (12). All astrocytes having visible cellular contacts exhibited functional coupling ($88 \pm 4.7\%$ recovery, $n = 17$), which could be completely and reversibly blocked by octanol (no recovery, $n = 7$) or halothane ($0.8 \pm$

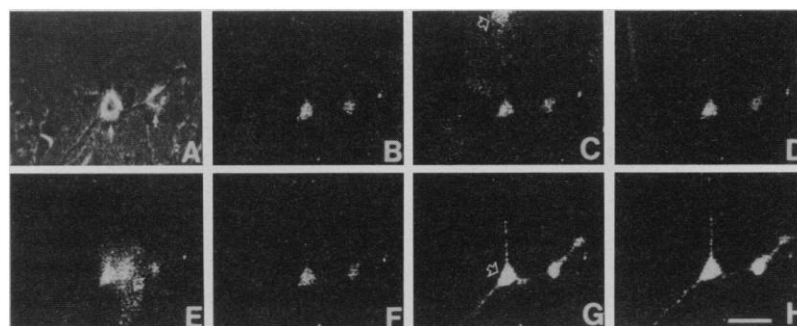


Fig. 4. Inhibition of astrocyte-to-neuron signaling by the gap junction blocker octanol. **(A)** Phase-contrast image of two neurons (small arrows) resting on a continuous layer of astrocytes (10 days in vitro). **(B)** Base line Ca^{2+} signal in the same field, in cells loaded with fluo-3. As $[\text{Ca}^{2+}]_i$ rises, the relative emission intensity of fluo-3 changes from black to white. **(C)** Electric field potential ($15 \mu\text{A}$ for 0.5 s) was first applied (open arrow) to the astrocyte lying beneath the upper neuronal process, in the presence of 0.5 mM octanol. A marked local increase in astrocytic $[\text{Ca}^{2+}]_i$ was evoked by 2 s . **(D)** The concentration of astrocytic Ca^{2+} returned to the base line without triggering an increase in neuronal $[\text{Ca}^{2+}]_i$ or a propagating Ca^{2+} wave (2 min). **(E)** The astrocyte subjacent to the neuron was subsequently stimulated (open arrow). Although astrocytic $[\text{Ca}^{2+}]_i$ increased (2 s), no neuronal response was evoked **(F)** (2 min). **(G)** Subsequent direct stimulation of the neuron ($5 \mu\text{A}$ for 0.5 s) evoked a large increase in neuronal $[\text{Ca}^{2+}]_i$, indicating that the lack of signal transmission was not a result of an impaired neuronal $[\text{Ca}^{2+}]_i$ response. Note the co-activation of the neuron to the right. **(H)** The concentration of neuronal Ca^{2+} did not return to a resting level within 2 min . Scale bar, $50 \mu\text{m}$.

0.7% recovery, $n = 10$). In contrast, neurons only partially regained fluorescence after photobleaching ($9.8 \pm 2.0\%$ recovery, $n = 29$), and this recovery occurred despite concurrent gap junction blockade with either octanol ($8.1 \pm 1.8\%$ recovery, $n = 7$) or halothane ($6.5 \pm 4.1\%$ recovery, $n = 9$). Thus, my experiments suggest that cultured neurons lack a significant degree of gap junction coupling either to one another or to local astrocytes. Consistent with this observation, Lucifer yellow injected into cultured neurons fails to spread into surrounding astrocytes (2). However, it is possible that unidirectional intercellular connections exist that are not detected by these dyes: the threshold for detecting Lucifer yellow dye-coupling between cells is estimated to be 2 nS , corresponding to roughly 20 functional gap junction channels (13). Lucifer yellow and biotin pass readily from astrocytes into adjacent oligodendrocytes and Müller cells of the intact retina, but rarely in the opposite direction. Thus, gap junctions with unidirectional diffusion capabilities might exist between heterogeneous cell types (14). The possibility of neuronal-glia asymmetric dye diffusion is suggested by the distinctly different gap junction proteins expressed by neurons and glia (13). Astrocytic gap junctions contain connexin 43, whereas neurons are immunoreactive for the gap junction protein connexin 32 (13). In addition, CA3 neurons of the hippocampus are coupled both electrically and by dye transfer studies (13). Also, extensive interneuronal coupling has been found with neurobiotin labeling of neocor-

tical columns in postnatal rodents (15).

My data demonstrate that Ca^{2+} signals can propagate from astrocytes to neurons and that astrocytes can thereby directly modulate neuronal $[\text{Ca}^{2+}]_i$. In addition, I have observed that Ca^{2+} signaling between astrocytes and neurons is unidirectional and is inhibited by the gap junction blocker octanol. This in vitro perturbation of neuronal $[\text{Ca}^{2+}]_i$ by local astrocytes challenges the general presumption that neurons alone are responsible for information processing in the central nervous system.

These in vitro observations may underlie the in vivo phenomenon of spreading depression (SD). Spreading depression is a slowly moving wave of tissue depolarization (18 to $50 \mu\text{m/s}$) that can be elicited by mechanical injury, electrical stimulation, or by application of K^+ and glutamate to exposed cortical tissue (16). Passive diffusion of K^+ or glutamate in the interstitial space has been proposed as a possible mechanism for the propagation of SD (17). It is possible, however, that SD travels as an intracellular Ca^{2+} wave in astrocytes. Consistent with this suggestion, halothane anesthesia inhibits both the elicitation and migration of SD (18), whereas TTX affects neither the propagation of SD nor the decline in interstitial Na^+ during SD (19).

REFERENCES AND NOTES

1. H. F. Cserr and M. Bundgaard, *Ann. N.Y. Acad. Sci.* **1**, 481 (1986).
2. J. W. Dani, A. Chernjavsky, S. J. Smith, *Neuron* **8**, 429 (1992); T. H. Murphy, L. A. Blatter, W. G. Wier, J. M. Baraban, *J. Neurosci.* **13**, 2672 (1993).

3. N. E. Reist and S. J. Smith, *Proc. Natl. Acad. Sci. U.S.A.* **89**, 7625 (1992); S. Kriegler and S. Y. Chiu, *J. Neurosci.* **13**, 4229 (1993).

4. A. H. Cornell-Bell, S. M. Finkbeiner, M. S. Cooper, S. J. Smith, *Science* **247**, 470 (1990); A. M. Jensen and S. Y. Chiu, *J. Neurosci.* **10**, 1165 (1990); A. C. C. Charles, J. E. Merrill, E. R. Dirksen, M. J. Sanderson, *Neuron* **6**, 983 (1991); S. Finkbeiner, *ibid.* **8**, 1101 (1992); A. C. C. Charles *et al.*, *J. Cell Biol.* **118**, 195 (1992).

5. Mixed forebrain cultures from embryonic rats were prepared as described [S. A. Goldman, W. A. Pulsinelli, W. Y. Clarke, R. P. Kraig, F. Plum, *J. Cereb. Blood Flow Metab.* **9**, 471 (1989)]. Cultures were grown 1 to 6 weeks in vitro before use. The cells were loaded with 10 μ M fluo-3 acetomethoxyester (fluo-3 AM; Molecular Probes) for 1 hour at 37°C. A Bio-Rad confocal scanning microscope MCR600 attached to an inverted microscope (Olympus IMT-2) was used for imaging of the fluo-3 signal. Excitation was provided by the 488-nm line of a 25-mW argon laser filtered to less than 1% by neutral density filters. Emission was long pass-filtered (515 nm) and detected with the confocal aperture set to its maximal opening (7 mm). Images were acquired every 0.5 to 3 s and recorded on a Panasonic TQ-2028F optical memory disk recorder. Relative changes in fluorescence were calculated and normalized against the base line fluorescence (F) by $\Delta F/F$. Background counts were subtracted from all measurements. Experiments were carried out at room temperature in Hanks balanced salt solution (HBSS; Gibco). For experiments performed with no extracellular Ca^{2+} , HBSS was exchanged for a similar solution containing no Ca^{2+} and 0.5 mM EGTA.

6. Focally applied electric fields were produced as described [N. B. Patel and M.-M. Poo, *J. Neurosci.* **4**, 2939 (1984); R. W. Davenport and S. B. Kater, *Neuron* **9**, 405 (1992)]. Constant current (dc) of 2 to 28 μ A was passed for 0.5 s between the micropipette and an Ag-AgCl ground electrode and monitored throughout the experiment. The current density, J , at a distance r from the electrode tip was calculated by

$$J = I/2\pi r^2$$

where I is the total current flow. Although in some experiments astrocytic Ca^{2+} waves were also elicited by either mechanical stimulation (briefly deforming the plasma membrane with the electrode tip) or by laser excitation, in several experiments laser stimulation caused an uncontrollable degree of fluo-3 bleaching, and mechanical stimulation often induced irreversible damage of the target cell. Therefore, in routine experiments astrocytic Ca^{2+} waves were elicited by electric field stimulation.

7. GFAP (G 9269; Sigma) and MAP-2 (clone AP-20; Sigma) staining were performed according to standard procedures [M. Nedergaard, S. A. Goldman, S. Desai, W. A. Pulsinelli, *J. Neurosci.* **11**, 2489 (1991)]. After staining, each culture was viewed by epifluorescence.

8. In routine experiments, a perfusion rate of 0.1 mm/s was used. In selected experiments, this perfusion rate was increased to 1 to 2 mm/s without affecting the intercellular Ca^{2+} wave.

9. Spontaneous synaptical activity is almost completely inhibited by this concentration of TTX [T. H. Murphy, L. A. Blatter, W. G. Wier, J. M. Baraban, *J. Neurosci.* **12**, 4834 (1992)].

10. B. Katz and R. Miledi, *J. Physiol. (London)* **189**, 407 (1967).

11. Cultures were loaded with fluo-3 and exposed to 100 μ M glutamate for 1 min in the presence of either 2 mM halothane or 0.5 mM octanol. The glutamate-induced increase in $[Ca^{2+}]_i$ was $344 \pm 206\%$ and $410 \pm 239\%$ in the presence and absence of octanol, respectively (24 neurons in four experiments), whereas $[Ca^{2+}]_i$ increased $255 \pm 205\%$ and $251 \pm 190\%$ after glutamate exposure in the presence and absence, respectively, of halothane (19 neurons in three experiments).

12. Cultures were incubated with 2 μ M dicarboxy-

dichlorofluorescein diacetate (CDCF) for 5 min and incubated in the absence of CDCF for another 30 min [M. Nedergaard, S. Desai, W. Pulsinelli, *Anal. Biochem.* **187**, 109 (1990)]. After a base line fluorescence image of the culture was obtained, the area of laser scanning was reduced to include only one target cell. Complete or almost complete photobleaching occurred after 10 to 20 scans, each lasting 1 s at full laser power. Subsequently, the microscope settings were returned to recording configuration, and the refill was monitored for 20 min [M. H. Wade, J. E. Trosko, M. Schindler, *Science* **232**, 525 (1986); S. M. Finkbeiner, *Neuron* **8**, 1101 (1992); J. Mantz, J. Cordier, C. Giaume, *Anesthesiology* **78**, 892 (1993)].

13. R. Dermietzel *et al.*, *Proc. Natl. Acad. Sci. U.S.A.* **86**, 10148 (1989); S. Shiosaka, T. Yamamoto, E. L.

Hertzberg, J. I. Nagy, *J. Comp. Neurol.* **281**, 282 (1989); R. Dermietzel and D. C. Spray, *Trends Neurosci.* **16**, 186 (1993).

14. S. R. Robinson, E. C. G. M. Hampson, M. N. Munro, D. I. Vaney, *Science* **262**, 1072 (1993); J. L. Flagg-Newton and W. R. Loewenstein, *ibid.* **207**, 771 (1980).

15. A. Peinado, R. Yuste, L. C. Katz, *Neuron* **10**, 103 (1993).

16. A. A. P. Leao, *J. Neurophysiol.* **7**, 359 (1944).

17. A. J. Hansen, *Physiol. Rev.* **65**, 101 (1985).

18. R. Saito *et al.*, *J. Cereb. Blood Flow Metab.* **13**, S86 (1993).

19. C. Tobiasz and C. Nicholson, *Brain Res.* **241**, 329 (1982).

17 November 1993; accepted 18 February 1994

Genetic Mapping of Quantitative Trait Loci for Growth and Fatness in Pigs

Leif Andersson,* Chris S. Haley, Hans Ellegren, Sara A. Knott, Maria Johansson, Kjell Andersson, Lena Andersson-Eklund, Inger Edfors-Lilja, Merete Fredholm, Ingemar Hansson, Jan Håkansson, Kerstin Lundström

The European wild boar was crossed with the domesticated Large White pig to genetically dissect phenotypic differences between these populations for growth and fat deposition. The most important effects were clustered on chromosome 4, with a single region accounting for a large part of the breed difference in growth rate, fatness, and length of the small intestine. The study is an advance in genome analyses and documents the usefulness of crosses between divergent outbred populations for the detection and characterization of quantitative trait loci. The genetic mapping of a major locus for fat deposition in the pig could have implications for understanding human obesity.

Quantitative genetic variation is the major determinant of intra- and interpopulation differences for many traits of biological, medical, and agricultural significance. Quantitative (or polygenic) inheritance implies that variation in the trait is determined by the action of alleles at several loci together with environmental factors. We have, however, only vague ideas about the

number, location, and action of loci controlling quantitative variation. Recently, the ability to dissect genetically quantitative traits has been improved by the development of detailed linkage maps based on DNA markers. With these the segregation of individual chromosome segments can be traced in appropriate pedigrees. Thus, quantitative trait loci (QTLs) segregating in crosses between inbred lines of tomato (1), rat (2), and maize (3) have been mapped. The statistical method used in these studies, maximum likelihood interval mapping (4), cannot be used in studies of most domesticated animal species because of the lack of inbred lines. However, an analytical method based on least squares for the identification of QTLs segregating in crosses between divergent outbred lines has been described (5). The present study is an experimental application of the method.

European domesticated pigs are thought to have been derived largely from the European wild boar, with some crossbreeding with Chinese domesticated breeds in the 18th to 19th centuries (6). Despite striking phenotypic differences between the wild boar and domesticated pigs, they are sufficiently closely related to interbreed easily. We generated a three-generation pedigree by crossing two European

L. Andersson, H. Ellegren, M. Johansson, K. Andersson, L. Andersson-Eklund, I. Edfors-Lilja, Department of Animal Breeding and Genetics, Swedish University of Agricultural Sciences, Box 7023, S-750 07 Uppsala, Sweden.

C. S. Haley, AFRC Roslin Institute (Edinburgh), Roslin, Midlothian, EH25 9PS, Scotland, and INRA Station de Génétique Quantitative et Appliquée, 78350 Jouy-en-Josas, France.

S. A. Knott, Institute of Cell, Animal, and Population Biology, University of Edinburgh, West Mains Road, Edinburgh, EH9 3JT, Scotland, and INRA Station de Génétique Quantitative et Appliquée, 78350 Jouy-en-Josas, France.

M. Fredholm, Department of Animal Production and Animal Health, Division of Animal Genetics, The Royal Veterinary and Agricultural University, 1870 Fredrikberg C, Denmark.

I. Hansson and K. Lundström, Department of Food Science, Swedish University of Agricultural Sciences, S-750 07 Uppsala, Sweden.

J. Håkansson, Department of Animal Nutrition and Management, Swedish University of Agricultural Sciences, S-750 07 Uppsala, Sweden.

*To whom correspondence should be addressed.